Cerebral Cortex, February 2017;27: 1216–1228

doi:10.1093/cercor/bhv308
Advance Access Publication Date: 18 December 2015
Original Article

ORIGINAL ARTICLE

The Corticocortical Structural Connectivity of the Human Insula

Jimmy Ghaziri[1,4], Alan Tucholka[4,5,6,8], Gabriel Girard[7], Jean-Christophe Houde[7], Olivier Boucher[2,8], Guillaume Gilbert[9], Maxime Descoteaux[7], Sarah Lippé[2,8], Pierre Rainville[2,10,3] and Dang Khoa Nguyen[1,4,11]

[1]Département de Neurosciences, [2]Centre de recherche en neuropsychologie et cognition, Département de Psychologie, [3]Département de Stomatologie, Université de Montréal, Montréal, QC, Canada, [4]Centre de Recherche du Centre Hospitalier de l'Université de Montréal, Montréal, QC, Canada, [5]BarcelonaBeta Brain Research Center, Pasqual Maragall Foundation, Barcelona, Spain, [6]Département de Radiologie, CHUM hôpital Notre-Dame, Montréal, QC, Canada, [7]Sherbrooke Connectivity Imaging Lab (SCIL), Computer Science department, Université de Sherbrooke, Sherbrooke, QC, Canada, [8]Centre de recherche du CHU Hôpital Sainte-Justine, Montréal, QC, Canada, [9]MR Clinical Science, Philips Healthcare, Cleveland, OH, USA, [10]Centre de Recherche de l'Institut Universitaire de Gériatrie de Montréal, Montréal, QC, Canada and [11]Service de Neurologie, CHUM Hôpital Notre-Dame, Montréal, QC, Canada

Address correspondence to Dang Khoa Nguyen, CHUM Hôpital Notre-Dame, Service de Neurologie, 1560 rue Sherbrooke Est, Montreal, QC H2L 4M1, Canada. Email: d.nguyen@umontreal.ca

Abstract

The insula is a complex structure involved in a wide range of functions. Tracing studies on nonhuman primates reveal a wide array of cortical connections in the frontal (orbitofrontal and prefrontal cortices, cingulate areas and supplementary motor area), parietal (primary and secondary somatosensory cortices) and temporal (temporal pole, auditory, prorhinal and entorhinal cortices) lobes. However, recent human tractography studies have not observed connections between the insula and the cingulate cortices, although these structures are thought to be functionally intimately connected. In this work, we try to unravel the structural connectivity between these regions and other known functionally connected structures, benefiting from a higher number of subjects and the latest state-of-the-art high angular resolution diffusion imaging (HARDI) tractography algorithms with anatomical priors. By performing an HARDI tractography analysis on 46 young normal adults, our study reveals a wide array of connections between the insula and the frontal, temporal, parietal and occipital lobes as well as limbic regions, with a rostro-caudal organization in line with tracing studies in macaques. Notably, we reveal for the first time in humans a clear structural connectivity between the insula and the cingulate, parahippocampal, supramarginal and angular gyri as well as the precuneus and occipital regions.

Key words: cingulate, diffusion, insula, insular cortex, tractography

Introduction

Located in the depth of the Sylvian fissure, the insula, a pyramidal-shaped structure, is considered as the fifth lobe of the brain (Stephani et al. 2011) and represents ~1%–4% of the total cortical surface (Semendeferi and Damasio 2000). Topographically, the insula is covered laterally by the frontal, parietal and temporal

opercula, while delimited medially by the extreme capsule, the claustrum, the external capsule (harboring the arcuate fasciculus), the lenticular nucleus and the internal capsule (Türe et al. 1999). It is divided by the central insular sulcus into an anterior portion comprising 3 to 4 short gyri, and a posterior portion composed of 2 long gyri (anterior and posterior), which form a fan-like pattern (Flynn 1999). It is also divided into 3 architectonic zones based on its organization, shape, number and type of neurons: 1) an agranular zone (Ia) located rostroventrally at the limen insulae; 2) a granular zone (Ig) positioned caudodorsally covering the dorsal posterior insula and in between; 3) a dysgranular transitional (or intermediate) zone (Id) spanning from the anterior to the posterior insula (Mesulam and Mufson 1985).

Cumulative work utilizing various techniques (electrophysiology, functional neuroimaging, and positron emission tomography) along with lesion studies in primates, including humans, has established a role for the insula in a wide array of functions, including autonomic functions, viscero-sensory and motor function, motor association, vestibular function, language, somatosensation, chemosensation, central audition, emotions, pain, bodily awareness, self-recognition, attention, empathy, time perception, motivation, craving, and addiction (for an extensive review, see Shelley and Trimble 2004; Kurth et al. 2010; Nieuwenhuys 2012). These studies have also revealed different functional profiles between the left versus the right insula and the anterior versus the posterior insula.

Seminal work on nonhuman primates have demonstrated widespread connections between the insula and the frontal, temporal, and parietal cortices, and limbic areas (Mesulam and Mufson 1982a,b; Mufson and Mesulam 1982; Vogt and Pandya 1987), consistent with the wide variety of functions associated with this structure (see Augustine 1996). In humans, however, the structural connectivity of the insula is less documented. Comparative studies have shown that the insula has undergone a gradual increase in the complexity of its organization and size in the course of primate and hominid evolution (Semendeferi and Damasio 2000; Bauernfeind et al. 2013). The anatomical organization of insular sulci in humans is different from that of nonhuman primates, and it has been suggested that the greater size of some regions is correlated with newly emerged specialized functions such as empathy and social awareness (Semendeferi and Damasio 2000; Allen et al. 2002; Kaas 2013). Moreover, von Economo neurons (VENs; for a review, see von Economo and Koskinas 1925; von Economo 1926; Cauda et al. 2014) have been reported in humans, great apes, and more recently macaques (Evrard et al. 2012). The implication of these neurons in its connectivity map is still poorly known but may play a role in a differential connectivity pattern (Cauda et al. 2014). Cross-species comparisons with humans have been challenging due to differences in investigative methods, such as tract-tracing that are not feasible on humans. However, recent developments in MRI-based diffusion-weighted imaging have made noninvasive study of structural connectivity possible in vivo with increasing precision and reliability.

To our knowledge, only 3 studies have investigated the structural connectivity of the human insula. Cloutman et al. (2012) recruited 24 subjects, scanned them using a 3Testla MRI and used a dedicated software package (PICo method) to run a probabilistic tractography algorithm with 20000 streamlines per voxel based on the Automated Anatomical Labeling atlas (Tzourio-Mazoyer et al. 2002). Cerliani et al. (2012) scanned 10 subjects on a 3Tesla MRI scan using FMRIB's toolbox and a probabilistic tractography algorithm with 5000 seeds per voxel. Jakab et al. (2012) scanned 40 subjects on a 1.5Testla MRI scan using FMRIB's toolbox and probabilistic tractography algorithm with 1 seed per voxel. Their results showed that the anterior insular cortex has connections with the orbitofrontal cortex, the inferior and superior temporal gyri, the temporal pole, the thalamus, and the amygdala; that the middle insular cortex has connections with the superior and inferior frontal gyri, the precentral, postcentral, and supramarginal gyri, the inferior and superior temporal gyri, the orbitofrontal and the parietal cortices, while the posterior insular cortex has connections with the superior and inferior frontal gyri, the precentral and postcentral gyri, the inferior and superior temporal gyri, the parietal cortex, and the putamen (reviewed in Ghaziri et al. 2014). Surprisingly, none of these studies reported connections with the cingulate gyrus, although these have been described in tracing studies in animals (Mesulam and Mufson 1982b; Mufson and Mesulam 1982) and functional studies in humans (Taylor et al. 2009; Cauda et al. 2011).

In light of these latter structural connectivity studies, which are based on DTI probabilistic tractography, standard templates, and a low number of subjects in some cases, our objective was to further investigate the connectivity of the insular cortex in humans. We put an emphasis on regions known to be related with the insula in nonhuman primates' studies as well as human functional studies such as the cingulate, parahippocampal, supramarginal, and angular gyri among others, by using the latest state-of-the-art tractography methods. To do so, we based our study on state-of-the-art HARDI deterministic tractography with anatomical priors similar to (Smith et al. 2012), recruited a significant number of subjects, while using random parcellation, in order to overcome known methodological limitations such as crossing-fibers, low resolution, and invalid connections as defined in Côté et al. (2013).

Materials and Methods

Participants

Forty-six healthy right-handed subjects between the age of 19 and 39 (mean age ± SD: 24.5 ± 4.8; 18 men and 28 women), with no history of neurological or psychiatric disorders, were recruited. Informed written consent was obtained from all participants for procedures approved by the Centre Hospitalier de l'Université de Montréal (CHUM) ethics board, in accordance with the latest revision of the declaration of Helsinki.

Data Acquisition

MRI data were acquired on a 3T Achieva scanner (Philips, the Netherlands). The diffusion-weighted images were acquired with a single-shot spin-echo echo-planar pulse sequence (TR = 7.96 ms; TE = 77 ms; flip angle = 90°; slices = 68; field of view = 230 mm; matrix = 128 × 128; voxel resolution = 1.8 × 1.8 × 1.8 mm; readout bandwidth = 19.6 Hz/pixels; echo-planar imaging direction bandwidth = 1572.5 Hz; 8-channel head coil; SENSE acceleration factor =2). One pure T_2-weighted image ($b = 0$ s/mm^2) and 60 images with noncollinear diffusion gradients ($b = 1500$ s/mm^2) were obtained. In addition, T_1-weighted images were acquired using 3D T_1 gradient echo (scan time = 8.11 min; TR = 8.1 ms; TE = 3.8 ms; flip angle = 8°; slices = 176; voxel size =1 × 1 × 1 mm, FOV 230 × 230 mm).

Analyses

Anatomical Images Preprocessing

Anatomical T_1-weighted images were preprocessed with the FMRIB's software library (FSL; v.5.0.1, http://fsl.fmrib.ox.ac.uk/

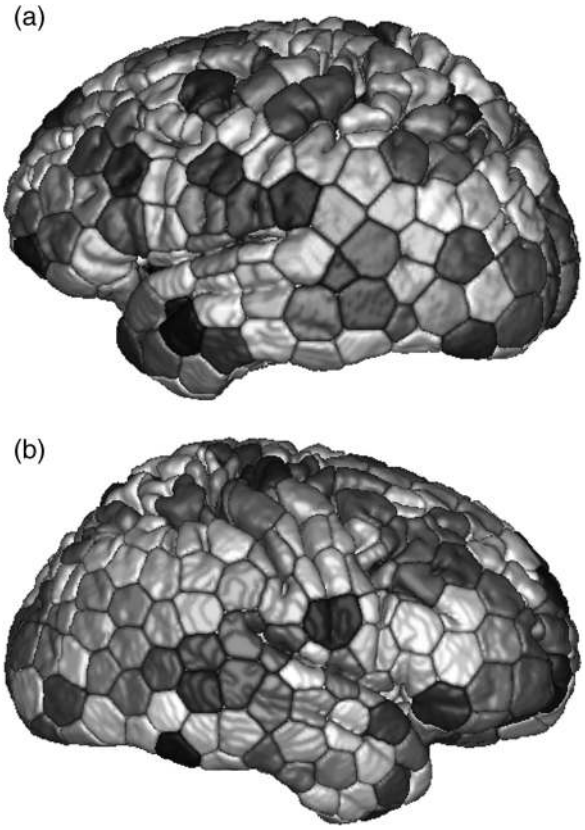

Figure 1. (*a*) Random parcellation of the left cortex into 200 regions (voronoï). (*b*) Random parcellation of the right cortex into 200 regions (voronoï).

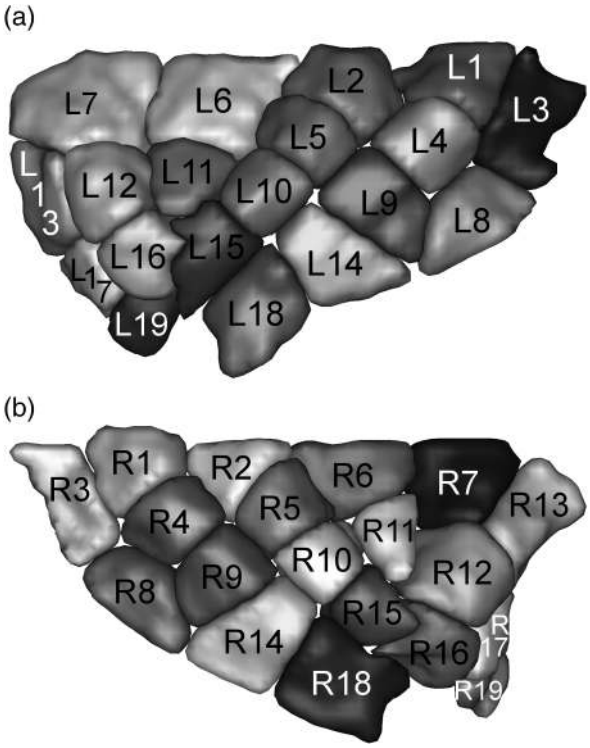

Figure 2. (*a*) Random parcellation of the left insula into 19 regions (voronoï). (*b*) Random parcellation of the right insula into 19 regions (voronoï).

fsl/fslwiki/FSL, last accessed November 27, 2015) (Smith et al. 2004; Woolrich et al. 2009; Jenkinson et al. 2012). The brain extraction tool (BET) (Smith 2002) was used to remove nonbrain tissues, after which images were segmented using FMRIB's automated segmentation tool (Zhang et al. 2001) resulting into probabilistic maps of white matter (WM), gray matter (GM), and cerebrospinal fluid (CSF) for each subject.

Template Creation

A template representing every subject in a unique referential space had to be created in order to generate a normalized parcellation of the cortex of each hemisphere. Advanced Normalization Tools (ANTS) (v. 1.5, http://stnava.github.io/ANTs/, last accessed November 27, 2015; Avants and Gee 2004; Klein et al. 2009; Avants et al. 2010) was used to create a template from our 46 anatomical T_1-weighted images using a bi-directional diffeomorphic algorithm, generating matrices to pass from the template space to each native subject space and *vice versa*. The probabilistic GM maps of each subject were then resampled to the template space using a linear interpolation. An average map of GM in the normalized space was then created, binarized, and manually cleaned to: 1) remove nonbrain tissue (segmentation, artifacts), 2) remove the cerebellum, 3) separate left and right hemisphere, and 4) delineate the insular cortex in each hemisphere. Manual segmentation was performed using ITK-SNAP software (v.2.4.0, http://www.itksnap.org, last accessed November 27, 2015; Yushkevich et al. 2006) and was double-checked by 2 different investigators.

Creation of the Regions of Interests

The binary cleaned cortex map of each hemisphere was randomly parcellated into 200 regions using a k-mean algorithm (Figs 1*a* and 2*b*). As for the insular cortex, each hemisphere was manually segmented by following a sulco-gyral division. Based on previous studies (Türe et al. 1999; Naidich et al. 2004; Tanriover et al. 2004; Afif et al. 2009; Afif and Mertens 2010; Cohen et al. 2010) and following the nomenclature of Türe et al. (1999), we first segmented the insula using a sagittal view, starting from the limit of the dorsal anterior insular point through the anterior periinsular sulcus. Ventro-laterally, we stopped at the level of the anterior transverse insular gyrus to draw the anterior short gyrus; ventro-medially, we stopped at the level of the junction between the internal and external capsule. We continued from there ventro-caudally toward the limen insula (at the limit of the temporal operculum) and the inferior periinsular sulcus, stopping at the posterior insular point caudally to draw the posterior long gyrus. We then segmented dorso-caudally from there at the limit of the superior periinsular to finish at the anterior insular point closing the superior part of the insula. We then separated the insula into an anterior and posterior region as delimited by the insular central sulcus. From an axial view, we started medially at the inferior periinsular sulcus, caudally, to the short insular sulcus, dorsally, passing at the junction of the external capsule and stopping laterally at the limit of the CSF in the Sylvian fissure.

Finally, centroids were regularly placed within each gyri and then simultaneously inflated, resulting in a parcellation into 19 regions (Figs 2*a* and *b*). The same technique was used for both hemispheres; the visible differences in each ROIs may be the result of interhemispheric differences. The voronoï-partitioning algorithm of the cortex and the number of insular ROIs was inspired from previous studies (Hagmann et al. 2007, 2008; Zalesky et al. 2010).

HARDI data Preprocessing

The preprocessing steps described in this paragraph have been done on each subject separately. We first applied eddy current

correction from FSL Diffusion Toolbox (FDT) to adjust the diffusion data for distortion and motion using affine registration to the nonweighted diffusion volume ($b = 0$ s/mm^2). We then applied a nonlocal means (NL-means) Rician denoising method on all diffusion-weighted volumes to increase image quality (Coupe et al. 2008). The resulting image was upsampled to a 1 mm resolution to better differentiate the insula, the claustrum, and the extreme capsule, as done in other HARDI tractography work (Raffelt et al. 2012; Smith et al. 2012; Girard et al. 2014). We performed a quality assurance on the resulting images by verifying the T_1-weighted white-matter mask and the red-green-blue (RGB) diffusion color map. Using BET from FSL on the $b = 0$ image, we extracted the brain and created a binary brain mask so the preprocessing on diffusion images is performed only on the brain. Diffusion tensors (Basser et al. 1994) and a fractional anisotropy (FA) map were created using MRtrix package (J-D Tournier, Brain Research Institute, Melbourne, Australia, http://www.brain.org.au/software/, last accessed November 27, 2015; Tournier et al. 2012). The FA map is used for verification purposes (Tournier et al. 2007) as the data are visually checked after each step. We use a white-matter probabilistic map, obtained from anatomical T_1-weighted image, in the tracking algorithm as it has been shown to produce richer and more accurate streamlines than a thresholded FA map (Girard et al. 2014). The coregistration between the T_1-weighted image and the resampled to 1-mm diffusion images was performed using ANTS affine registration (Avants et al. 2011). The ROIs of the cortex and the insula were then resampled to every single-subject diffusion space. To check the validity of the registration from the template to individual diffusion space, we manually segmented 5 random subjects following the boundaries previously described and used 2 overlap agreement measures described in Klein et al. (2009) to compare the templates segmentation with these 5 subjects. We obtained an overlap of 82% and 86% for the "target overlap" and the "dice coefficient," respectively (Dice 1945).

Constrained spherical deconvolution (CSD) (Tournier et al. 2007; Descoteaux et al. 2009) computation was performed using MRtrix (Tournier et al. 2012) to resolve crossing-fibers more effectively while supporting more effectively noise effects (Tournier et al. 2008). Thereby, streamline tracking was launched on resulted fiber orientation distribution functions (fODF) (Tournier et al. 2007; Descoteaux et al. 2009) using a deterministic tractography algorithm (Girard et al. 2014) with a threshold of 150 seeds per voxel from all 19 ROIs of the insula and 200 ROIs of the cortex in both hemispheres. Because tractography cannot determine the orientation of a fiber, whether it is afferent or efferent, and

Table 1 Connectivity between the ROIs of the left insula and the left ROIs of the cortex with a threshold of 150 fibers per voxel

Regions	L1	L2	L3	L4	L5	L6	L7	L8	L9	L10	L11	L12	L13	L14	L15	L16	L17	L18	L19
Frontal lobe																			
Superior frontal gyrus	X	X			X	X	X	X		X	X	X	X	X	X	X			
Middle frontal gyrus	X	X			X	X	X	X			X	X		X					
Inferior frontal gyrus						X	X	X			X								
Orbital frontal cortex	X				X	X	X	X	X		X	X	X	X	X	X	X	X	X
Pars triangularis						X	X	X			X	X	X	X	X	X		X	
Pars opercularis		X				X	X	X			X	X							
Precentral gyrus	X	X	X	X	X	X	X	X	X	X				X					
Frontal opercula	X	X				X	X					X	X		X	X	X	X	
Frontal pole	X					X	X	X			X	X	X	X	X	X	X	X	
Parietal lobe																			
Superior parietal lobule	X		X	X				X	X					X					
Postcentral gyrus	X	X	X	X	X			X	X					X					
Supramarginal gyrus	X	X	X	X		X	X	X	X					X					
Angular gyrus			X					X						X					
Parietal opercula	X	X	X	X		X	X	X	X				X	X					
Precuneus			X					X						X					
Temporal lobe																			
Superior temporal gyrus	X	X	X			X	X	X					X	X	X	X	X	X	X
Planum temporale	X	X	X	X		X	X	X	X				X	X					
Planum polare	X	X	X			X		X	X	X			X	X	X	X	X	X	X
Heschl's gyrus	X	X	X	X		X	X	X	X					X			X	X	
Middle temporal gyrus	X		X				X	X					X	X	X	X	X	X	X
Inferior temporal gyrus							X						X	X		X	X	X	X
Temporal fusiform gyrus	X		X	X													X	X	X
Temporal pole		X		X	X	X	X	X	X	X	X		X	X	X	X	X	X	X
Occipital lobe																			
Lateral occipital cortex			X					X	X					X					
Cuneus			X																
Lingual				X														X	
Occipital fusiform gyrus																			
Occipital pole								X						X					
Limbic regions																			
Anterior parahippocampal gyrus					X				X	X		X			X	X	X	X	X
Posterior parahippocampal gyrus	X		X	X	X				X										
Anterior cingulate gyrus	X	X			X	X	X	X		X	X	X	X	X	X	X	X	X	X
Posterior cingulate gyrus		X	X											X					

because the path and angle of the tracts will differ depending on its starting point, we launched the tractography algorithm from both the insula and the cortex. After running the tractography algorithm on 5 random subjects with different thresholds ranging from 1 to 10 000 seeds per voxel, we observed a plateau of ~6000 streamlines with 300–400 seeds per voxels. Taking into consideration the computational power and time required for analysis, we elected to choose a threshold of 150 seeds per voxel which provided us with at least 5000 streamlines for every ROIs (very close to the plateau of 6000 streamlines). We used the probabilistic subject's GM map as an inclusion parameter, and the CSF and nonbrain voxels as an exclusion parameter; the step size was 0.5 mm; as described in Girard et al. (2014).

Normalization

To account for the difference in size of the ROIs, we normalized connectivity values relatively to the biggest ROI. Then, because tractography algorithm is not bijective, we summed each connection with its inverse for a better estimation of the real connectivity between each pair of ROIs.

Visualization

The template representing the 46 T_1-weighted images, the 19 insula ROIs of each hemisphere, and the cortex ROIs were affine-aligned to the Montreal Neurological Institute (MNI) 152 standard space. The regions were identified using the following *FSLview* integrated atlases: Harvard-Oxford cortical structural atlas (Frazier et al. 2005; Desikan et al. 2006; Makris et al. 2006; Goldstein et al. 2007), the MNI structural atlas (Collins et al. 1995; Mazziotta et al. 2001), and an atlas based on functional correlations (Tamraz et al. 2004).

Results

Connectivity Profile of the Insula

Bijective cortical connections of the 19 insular ROIs, with a threshold of 150 streamlines per voxel, are reported in Table 1 (for the left hemisphere) and Table 2 (for the right hemisphere). These results are also illustrated in Figure 3*a* (left hemisphere) and *b* (right hemisphere) and a general tractography illustration on one random subject is shown in Figure 4 for schematic

Table 2 Connectivity between the ROIs of the right insula and the right ROIs of the cortex with a threshold of 150 fibers per voxel

Regions	R1	R2	R3	R4	R5	R6	R7	R8	R9	R10	R11	R12	R13	R14	R15	R16	R17	R18	R19
Frontal lobe																			
Superior frontal gyrus		X			X	X	X	X		X	X	X	X	X	X				
Middle frontal gyrus		X			X	X	X			X	X	X	X						
Inferior frontal gyrus		X				X	X	X			X	X	X		X	X	X		
Orbital frontal cortex	X	X	X			X	X		X	X	X	X	X	X	X	X	X	X	X
Pars triangularis						X	X					X	X		X	X	X		
Pars opercularis		X				X	X	X			X	X	X						
Precentral gyrus	X	X	X	X	X	X	X	X	X	X				X					
Frontal opercula		X				X	X					X				X	X		
Frontal pole	X	X	X			X	X	X			X	X	X	X	X	X	X	X	X
Parietal lobe																			
Superior parietal lobule	X			X				X	X					X					
Postcentral gyrus	X	X	X	X	X			X	X	X				X					
Supramarginal gyrus	X	X	X	X			X	X	X				X						
Angular gyrus	X	X				X	X	X	X				X	X					
Parietal opercula	X	X	X	X	X	X	X	X	X	X			X						
Precuneus			X					X											
Temporal lobe																			
Superior temporal gyrus	X	X	X		X	X	X							X		X	X	X	X
Planum temporale	X	X	X	X	X	X	X	X	X	X			X						
Planum polare		X	X		X	X		X						X		X	X	X	X
Heschl's gyrus	X	X	X	X	X	X	X	X	X	X			X	X					
Middle temporal gyrus	X	X	X				X	X						X			X	X	X
Inferior temporal gyrus														X		X	X	X	X
Temporal fusiform gyrus														X		X		X	X
Temporal pole						X		X	X				X	X		X	X	X	X
Occipital lobe																			
Lateral occipital cortex			X	X			X	X	X					X					
Cuneus								X											
Lingual																	X	X	
Occipital fusiform gyrus								X						X				X	
Occipital pole								X						X			X	X	
Limbic regions																			
Anterior parahippocampal gyrus		X		X										X				X	
Posterior parahippocampal gyrus																			
Anterior cingulate gyrus		X			X	X	X			X	X	X	X	X	X	X	X	X	X
Posterior cingulate gyrus	X	X	X					X											

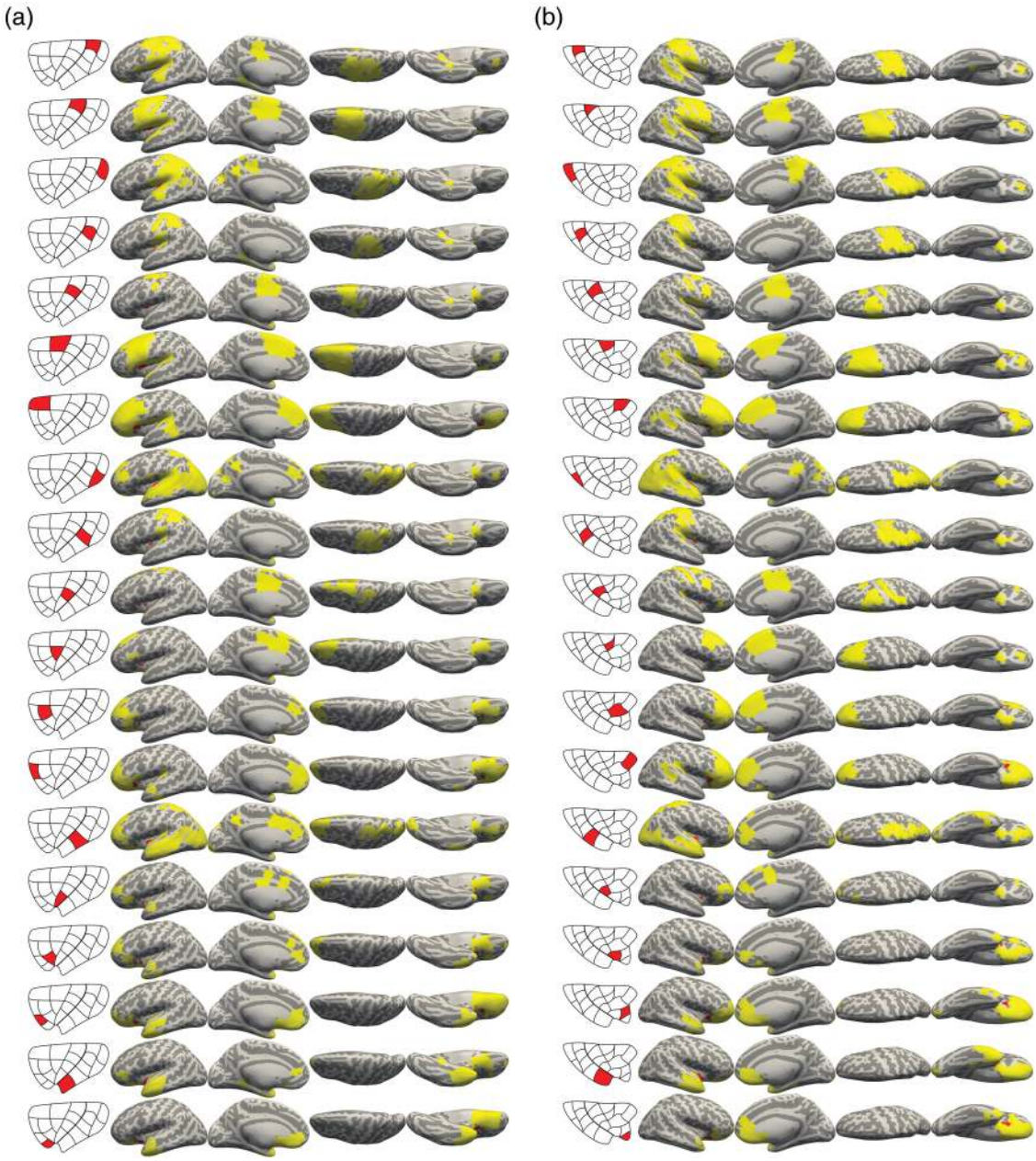

Figure 3. (*a*) Connectivity between the left insula and cortical ROIs with a threshold of 150 tracts per voxel. (*b*) Connectivity between the right insula and cortical ROIs with a threshold of 150 tracts per voxel.

purposes. Furthermore, in order to obtain a broadband connectivity map of the insula, we created a supplementary figure reflecting the connections ranging from 50 to 500 streamlines per voxel (Fig. 5*a* for the left hemisphere and *b* for the right hemisphere). As can be seen, the insula shows connections with the frontal, parietal, temporal, and occipital lobes, and limbic areas.

Widespread connections are observed between the insula and the frontal lobe. Insular ROIs from both hemispheres are connected with the inferior, including pars triangularis and orbitalis (Broca's area), middle, and superior frontal gyri, orbitofrontal cortex, precentral gyrus, frontal operculum, and subcallosal gyrus. With regards to the temporal lobe, the insula has connections with the superior temporal gyrus including Heschl's gyrus (auditory cortex), the planum temporale (Wernicke's area and associative auditory cortex), the planum polare, the temporal fusiform gyrus, and the temporal operculum. Within the parietal lobe, the insula has connections with the supramarginal and angular gyri, the precuneus and the superior parietal lobule, as well as the postcentral gyrus (somatosensory cortex; BA 1, 2, 3) and the parietal operculum. Within the occipital lobe, the insula has connections with the cuneus and lingual gyri, occipital fusiform gyrus, while including the lateral occipital cortex. Within limbic areas, the insula has connections with the parahippocampal gyrus, including the uncus, perirhinal and entorhinal cortices, and the anterior and posterior cingulate gyrus. More precisely, we report fibers connecting the anterior regions of the insula with the anterior cingulate cortex (BA 24), the anterior midcingulate cortex (BA 24, 32, 33), the subgenual subregion

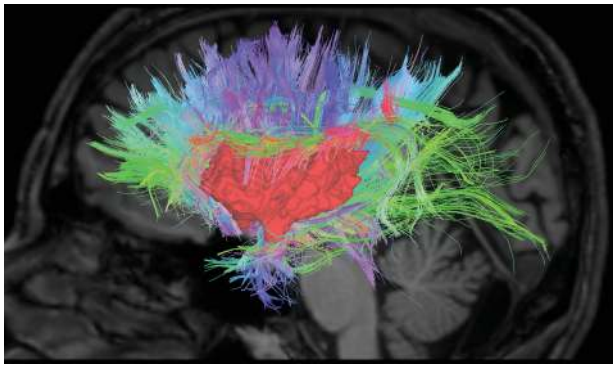

Figure 4. Streamlines from the insula to the cortex on a random subject with a threshold of 150 streamlines per voxel for illustrative purposes. Colors: Red: left-right; green: back-front; blue: up-down.

(BA 25), and the perigenual anterior cingulate cortex (BA 24, 32), while posterior regions of the insula are connected with the dorsal posterior cingulate cortex (BA 31) and the posterior midcingulate cortex (BA24, 33). We also found connections between the insula and the parahippocampal gyrus (anterior and posterior regions) including the entorhinal (BA28, 34) and perirhinal cortices (BA 35, 36), as well as the Uncus (BA 28).

Most of the reported regions with a threshold of 150 streamlines per voxels are still present with a higher threshold (up to 500, in yellow) (Fig. 4*a* and *b*). Indeed, many key regions are still connected in both hemispheres, including the superior and inferior temporal gyri, the anterior and posterior cingulate gyri, the precentral, postcentral, supramarginal, and angular gyri, the orbitofrontal as well as the occipital cortices.

We also observe a rostro-caudal like connectivity pattern as rostro-dorsal anterior ROIs are mainly connected to frontal and temporal lobes while ventro-caudal posterior like ROIs are mostly connected to temporal, parietal and occipital lobes (see Table 3).

Discussion

Our work reveals a wide array of connections between the insula and the frontal, temporal, and parietal lobes, and limbic areas, in agreement with tracing studies in macaques (Pandya et al. 1981; Mesulam and Mufson 1982a,b; Mufson and Mesulam 1982; Vogt and Pandya 1987; Vogt et al. 1987), structural (Cerliani et al. 2012; Cloutman et al. 2012; Jakab et al. 2012), and resting-state functional magnetic resonance imaging (rsfMRI) (Mutschler et al. 2009; Taylor et al. 2009; Van Den Heuvel et al. 2009; Cauda et al. 2011; Deen et al. 2011) studies in humans. Notably, the insula showed connections with the orbitofrontal cortex, supplementary motor area, frontal operculum, the primary motor and the somatosensory cortices, the parietal operculum, the auditory cortex, the prorhinal and entorhinal cortices (part of the anterior parahippocampal gyrus). This connectivity profile remains relatively stable by moving the standard threshold of 150 seeds per voxel to a more robust threshold of 500. A clear differential connectivity pattern, moving from a ventral anterior to a dorsal posterior organization, was observed. Remarkably, we were also able to reveal for the first time in humans clear structural connectivity between the insular cortex and cingulate cortex as well as the parahippocampal, angular, supramarginal, precuneus, cuneus, lingual and the fusiform gyri by overcoming known methodological limitations such as crossing-fibers (i.e., corona radiata) (Dougherty et al. 2005), and invalid connections (i.e., DTI-based probabilistic approach) (Yo et al. 2009). We suggest that we overcame, to some degree, crossing-fibers limitations by using high resolution data (1 mm) and HARDI with fODF compared with standard DTI tractography (2 mm) (Descoteaux et al. 2009; Jones et al. 2013; Kuhnt et al. 2013). Indeed, using anatomical priors results in having more valid connections and less invalid connections that end prematurely in the WM or stop in ventricles and does not connect cortical or subcortical areas. The particle filtering tractography algorithm also allows better propagation in narrow and tight white-matter band, which can be important in the complex areas surrounding the insula (Girard et al. 2014). Because of these methodological steps to minimize stray streamlines and artifacts, we surmise that obtained images represent actual connections. The fact that observed connections (e.g., cingulate, angular, supramarginal, lingual and parahippocampal gyri as well as precuneus and occipital cortex) are very much in line with cumulative data from tract-tracing studies in macaques (Mesulam and Mufson 1982b; Mufson and Mesulam 1982), functional studies in humans (Mutschler et al. 2009; Taylor et al. 2009; Van Den Heuvel et al. 2009; Cauda et al. 2011; Deen et al. 2011), and the limited number of tractography studies of the human insula (Cerliani et al. 2012; Cloutman et al. 2012; Jakab et al. 2012) is reassuring. As for the parahippocampal gyrus, its structural connectivity is poorly known and only a few studies have reported connections with the insula in rhesus monkeys and rats (Room and Groenewegen 1986; Insausti et al. 1987; Blatt et al. 2003; Kerr et al. 2007). One can speculate that the failure to observe the connectivity between the insula and the parahippocampal gyrus may be a result of the same limitations that apply for the cingulate cortex considering that it is part of a subcortical region encompassing a multitude of white-matter tracts (i.e., cingulum) (Catani and Thiebaut de Schotten 2008).

Cingulate Cortex

Although prior structural studies in humans have not revealed connections between the insula and cingulate cortex, a wide range of functional studies using rsfMRI have reported simultaneous activation of these 2 regions (Taylor et al. 2009; Van Den Heuvel et al. 2009; Cauda et al. 2011; Deen et al. 2011; Chang et al. 2013). Here, we show that there is indeed a direct connection between the insula and the cingulate cortex and that their functional co-activation, previously reported by rsfMRI, is a reflection of this direct link. In addition, the revealing of the antero-posterior pattern of structural connectivity between both structures is also in line with functional connectivity patterns reported in earlier rsfMRI studies: While the anterior insula is mainly connected with the anterior cingulate cortex, the posterior insula is preferentially connected with the posterior cingulate cortex (Cauda et al. 2011; Cerliani et al. 2012; Cloutman et al. 2012; Jakab et al. 2012). This strong link between both structures is further supported by the fact that their shared organization type (Vogt et al. 1995; Eickhoff et al. 2010), their neurons, such as VENs (Nimchinsky et al. 1995; Allman et al. 2011; Butti et al. 2013), and their shared functions (Torta and Cauda 2011).

Occipital Lobe

In accordance with previous structural (Cloutman et al. 2012; Jakab et al. 2012) and functional studies (Menon and Uddin 2010; Uddin et al. 2010; Cauda et al. 2011), we also report connections with the occipital lobe. An occipital connection might be plausible in pair with the claustrum due to their proximity (for a review, see Mathur 2014) along the external capsule, the

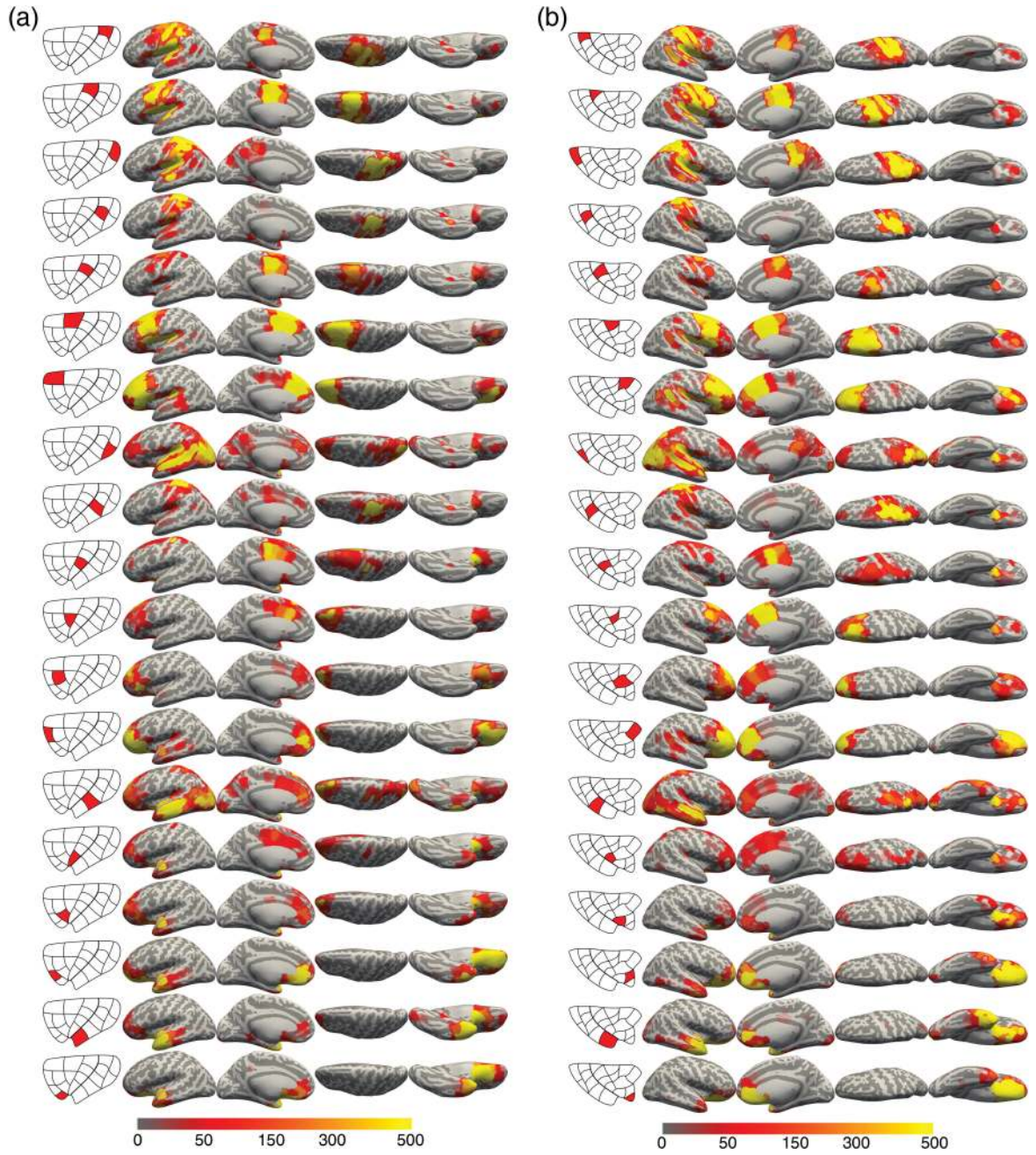

Figure 5. (*a*) Connectivity between the left insula and cortical ROIs with a threshold ranging from 50 (red), 150 (orange) to 500 (yellow) tracts per voxel. (*b*) Connectivity between the right insula and cortical ROIs with a threshold ranging from 50 (red), 150 (orange) to 500 (yellow) tracts per voxel.

uncinate fascicles, the corona radiata (Nieuwenhuys et al. 1988; Fernández-Miranda et al. 2008), or the inferior fronto-occipital fasciculus (IFOF) (Martino et al. 2010). Indeed, the claustrum and the parieto-occipital regions have been reported to have direct connections in animals (Mesulam and Mufson 1982b; Shipp et al. 1998; Tanné-Gariépy et al. 2002; Crick and Koch 2005) and humans (Schmahmann and Pandya n.d.; Schmahmann et al. 2007; Catani and Thiebaut de Schotten 2008). In addition, the IFOF, which is reported to be located underneath the insula and may be involved in the semantic system, has been shown to have connections with the temporal, parietal, and occipital lobes (Martino et al. 2010).

Related Insular Functions

The widespread connections found between the insula and other cortical regions are consistent with the wide range of brain functions associated with this structure and with the variety of neuropsychological impairments reported in patients with isolated insular damage. Insular connections with the frontal lobe are congruent, among others, with an insular involvement in language processes including speech initiation and complex articulation (Dronkers 1996; Bates et al. 2003; Boucher et al. 2015), and with high-order executive processes involving an affective component, such as risky decision-making (Clark et al. 2008; Weller et al. 2009). Connections with auditory areas in the temporal

Table 3 Rostro-caudal connectivity pattern of the left and right hemispheres

ROIs	Directionality	Lobes	ROIs	Directionality	Lobes
L1	Dorsal posterior	Frontal, temporal, and parietal	R1	Dorsal posterior	Frontal, temporal, and parietal
L2	Dorsal posterior	Frontal and temporal	R2	Dorsal posterior	Frontal, temporal, and parietal
L3	Dorsal posterior	Temporal, parietal, and occipital	R3	Dorsal posterior	Frontal, temporal, parietal, and occipital
L4	Dorsal posterior	Temporal and parietal	R4	Dorsal posterior	Frontal, temporal, parietal, and occipital
L5	Dorsal anterior	Frontal	R5	Dorsal anterior	Frontal, temporal ,and parietal
L6	Dorsal anterior	Frontal and temporal	R6	Dorsal anterior	Frontal, temporal, and parietal
L7	Dorsal anterior	Frontal and temporal	R7	Dorsal anterior	Frontal, temporal, parietal, and occipital
L8	Dorsal posterior	Frontal, temporal, parietal, and occipital	R8	Dorsal posterior	Frontal, temporal, parietal, and occipital
L9	Dorsal posterior	Frontal and temporal	R9	Dorsal posterior	Frontal, temporal, parietal, and occipital
L10	Dorsal anterior	Frontal and parietal	R10	Dorsal anterior	Frontal, temporal, and parietal
L11	Dorsal anterior	Frontal	R11	Dorsal anterior	Frontal
L12	Dorsal anterior	Frontal	R12	Dorsal anterior	Frontal
L13	Dorsal anterior	Frontal and temporal	R13	Dorsal anterior	Frontal, temporal, and parietal
L14	Ventral posterior	Frontal, temporal, parietal, and occipital	R14	Ventral posterior	Frontal, temporal, parietal, and occipital
L15	Ventral anterior	Frontal and temporal	R15	Ventral anterior	Frontal
L16	Ventral anterior	Frontal and temporal	R16	Ventral anterior	Frontal and temporal
L17	Ventral anterior	Frontal and temporal	R17	Ventral anterior	Frontal, temporal, and occipital
L18	Ventral posterior	Frontal and temporal	R18	Ventral posterior	Frontal, temporal, and occipital
L19	Ventral anterior	Frontal and temporal	R19	Ventral anterior	Frontal and temporal

lobe might explain the variety of central auditory deficits observed in patients with isolated insular damage (Bamiou et al. 2006), whereas those with parietal areas may be responsible for the hemispatial neglect and impaired body scheme representation described in some patients (Manes et al. 1999; Karnath et al. 2005; Golay et al. 2008). The insula and cingulate cortex have also been associated with similar neuropsychological functions, including self-awareness and representation of time and space, empathy, pain, and social behavior (Torta and Cauda 2011; Cauda et al. 2013, 2014), as well as being part of a salience or frontoparietal network (Seeley et al. 2007; Vincent et al. 2008; Menon and Uddin 2010). Similarly, the precuneus (Cavanna and Trimble 2006; Cabanis et al. 2013) and the supramarginal gyrus have been reported to be implicated in empathy and self-awareness. Finally, insular-occipital connections (cuneus and lingual gyrus), although somewhat less consistent with the literature, might be consistent with the impairment in facial emotional expression recognition following insular damage (Dal Monte et al. 2013) and may also be supported by functional studies on illusory own-body perception and self-perception, as well as word recognition among others (Karnath and Baier 2010; Craig 2011; Chiarello et al. 2013; Heydrich and Blanke 2013).

The insula seems to be part of the salience network (SN), which is formed by the dorsal anterior cingulate cortex (dACC) and the insular cortex with robust connectivity to subcortical and limbic structures (Seeley et al. 2007; Cauda et al. 2012; Ham et al. 2013). It has also been suggested that the 2 insular cortices have different patterns of functional connectivity. The anterior part of the SN is right sided and has stronger connections with the right AIC, right ACC, and many subcortical structures such as the brainstem, pons, and thalamus. The posterior part, which is the visuomotor integration network, has mild right sided connections with the superior temporal cortex and the occipital cortex (Cauda et al. 2011).

Limitations

The major limitation in our study is of technical nature, related to the diffusion-weighted imaging (DWI) tractography itself. While problems ensuing from false-negatives and crossing-fibers are reduced when using HARDI and CSD, we cannot completely exclude that some of the connecting fibers identified were crossing-fibers unrelated to the insula. As shown in Côté et al. (2013), probabilistic tracking with a large number of seeds produces a lot more invalid connections than corresponding HARDI deterministic tracking. Since the insula is a complex structure with a large number of crossing-fibers, we preferred to stay more conservative and use a deterministic tracking algorithm. In addition, typical DWI limitations persist in our study. These include the lack of standard criterion (i.e., threshold value and streamlines number) (for a review, see Dell'Acqua and Catani 2012), and a persistent low spatial resolution (even at $1 \times 1 \times 1$ mm) of the claustrum, as well as the distance effect (Morris et al. 2008). Furthermore, it cannot distinguish between afferent and efferent projections unlike tract-tracing injection (Johansen-Berg and Behrens 2006), posing a significant challenge to finding intraconnections of the insula. Moreover, diffusion tractography analysis cannot be run on the template image; therefore, any registration method from the template to the subject's space has its own methodological limitation. For example, the b0 to T_1 registration can result in slight mislocation of anatomy due to distortions. Indeed, because of MRI resolution limitations, it is possible that a few voxels of ventro-posterior ROIs of the insula include parts of the claustrum and that a few voxels of ventro-rostral anterior ROIs of the insula include parts of the orbitofrontal cortex.

Lastly, the atlases used to extract the connected regions are limited by their lack of standardized nomenclature and the omission of some regions.

Conclusion

Contrary to the current tractography-based connectivity of the insula literature, our work is based on a larger sample ($n = 46$) and uses the latest state-of-the-art HARDI tractography based on anatomical priors as described in the methodology. Our results show novel and clear connections between the insula and the cingulate, fusiform, parahippocampal, angular and supramarginal gyri as well as the precuneus and to a lesser extent with the cuneus and lingual gyrus. Hence, our results provide a structural basis to fundamental functions such as pain, empathy,

emotion, face recognition, interoception, language, social behavior, etc. Considering the brain is organized like a "small-world" network (Bianchi et al. 2012), these results help to further the understanding of the functional role the insula plays as a multimodal structure. Moreover, the continuous improvements of tractography techniques may help further investigate subcortical regions such as the hippocampus, the amygdala, the thalamus, and the striatum, providing the opportunity to compare structural interhemispheric connectivity. Consequently, a comparative study with clinical patients might also be beneficial.

Funding

This study was supported by Quebec Bio-Imaging Network (RBIQ/QBIN) # 4.11 and The Fondation du CHUM.

Notes

The authors would like to thank Prof. Mario Beauregard for sharing some data with us and the staff of the Neuroimaging Unit at Centre Hospitalier de l'Université de Montréal (CHUM, Hôpital Notre-Dame) for their technical assistance. In memory of Jean-Maxime Leroux. *Conflict of interests*: None declared.

References

Afif A, Hoffmann D, Becq G, Guenot M, Magnin M, Mertens P. 2009. MRI-based definition of a stereotactic two-dimensional template of the human insula. Stereotact Funct Neurosurg. 87:385–394.

Afif A, Mertens P. 2010. Description of sulcal organization of the insular cortex. Surg Radiol Anat. 32:491–498.

Allen JS, Damasio H, Grabowski TJ. 2002. Normal neuroanatomical variation in the human brain: an MRI-volumetric study. Am J Phys Anthropol. 118:341–358.

Allman JM, Tetreault NA, Hakeem AY, Park S. 2011. The von economo neurons in apes and humans. Am J Hum Biol. 23:5–21.

Augustine JR. 1996. Circuitry and functional aspects of the insular lobe in primates including humans. Brain Res Brain Res Rev. 22:229–244.

Avants B, Gee JC. 2004. Geodesic estimation for large deformation anatomical shape averaging and interpolation. Neuroimage. 23:139–150.

Avants BB, Tustison NJ, Song G, Cook PA, Klein A, Gee JC. 2011. A reproducible evaluation of ANTs similarity metric performance in brain image registration. Neuroimage. 54:2033–2044.

Avants BB, Yushkevich P, Pluta J, Minkoff D, Korczykowski M, Detre J, Gee JC. 2010. The optimal template effect in hippocampus studies of diseased populations. Neuroimage. 49:2457–2466.

Bamiou D-E, Musiek FE, Stow I, Stevens J, Cipolotti L, Brown MM, Luxon LM. 2006. Auditory temporal processing deficits in patients with insular stroke. Neurology. 67:614–619.

Basser PJ, Mattiello J, LeBihan D. 1994. MR diffusion tensor spectroscopy and imaging. Biophys J. 66:259–267.

Bates E, Wilson SM, Saygin AP, Dick F, Sereno MI, Knight RT, Dronkers NF. 2003. Voxel-based lesion-symptom mapping. Nat Neurosci. 6:448–450.

Bauernfeind AL, de Sousa AA, Avasthi T, Dobson SD, Raghanti MA, Lewandowski AH, Zilles K, Semendeferi K, Allman JM, Craig AD (Bud), et al. 2013. A volumetric comparison of the insular cortex and its subregions in primates. J Hum Evol. 64:263–279.

Bianchi MT, Klein JP, Caviness VS, Cash SS. 2012. Synchronizing bench and bedside: A clinical overview of networks and oscillations. In: Bianchi MT, Caviness VS, Cash SS, editors. Network approaches to diseases of the brain. Massachusetts: Bentham Science Publishers. p. 3–12.

Blatt GJ, Pandya DN, Rosene DL. 2003. Parcellation of cortical afferents to three distinct sectors in the parahippocampal gyrus of the rhesus monkey: an anatomical and neurophysiological study. J Comp Neurol. 466:161–179.

Boucher O, Rouleau I, Escudier F, Malenfant A, Denault C, Charbonneau S, Finet P, Lassonde M, Lepore F, Bouthillier A, et al. 2015. Neuropsychological performance before and after partial or complete insulectomy in patients with epilepsy. Epilepsy Behav. 43:53–60.

Butti C, Santos M, Uppal N, Hof PR. 2013. Von Economo neurons: clinical and evolutionary perspectives. Cortex. 49:312–326.

Cabanis M, Pyka M, Mehl S, Müller BW, Loos-Jankowiak S, Winterer G, Wölwer W, Musso F, Klingberg S, Rapp AM, et al. 2013. The precuneus and the insula in self-attributional processes. Cogn Affect Behav Neurosci. 13:330–345.

Catani M, Thiebaut de Schotten M. 2008. A diffusion tensor imaging tractography atlas for virtual in vivo dissections. Cortex. 44:1105–1132.

Cauda F, Costa T, Torta DME, Sacco K, D'Agata F, Duca S, Geminiani G, Fox PT, Vercelli A. 2012. Meta-analytic clustering of the insular cortex. Characterizing the meta-analytic connectivity of the insula when involved in active tasks. Neuroimage. 62:343–355.

Cauda F, D'Agata F, Sacco K, Duca S, Geminiani G, Vercelli A. 2011. Functional connectivity of the insula in the resting brain. Neuroimage. 55:8–23.

Cauda F, Geminiani GC, Vercelli A. 2014. Evolutionary appearance of von Economo's neurons in the mammalian cerebral cortex. Front Hum Neurosci. 8:104.

Cauda F, Torta DME, Sacco K, D'Agata F, Geda E, Duca S, Geminiani G, Vercelli A. 2013. Functional anatomy of cortical areas characterized by von Economo neurons. Brain Struct Funct. 218:1–20.

Cavanna AE, Trimble MR. 2006. The precuneus: a review of its functional anatomy and behavioural correlates. Brain. 129:564–583.

Cerliani L, Thomas RM, Jbabdi S, Siero JCW, Nanetti L, Crippa A, Gazzola V, D'Arceuil H, Keysers C. 2012. Probabilistic tractography recovers a rostrocaudal trajectory of connectivity variability in the human insular cortex. Hum Brain Mapp. 33:2005–2034.

Chang LJ, Yarkoni T, Khaw MW, Sanfey AG. 2013. Decoding the role of the insula in human cognition: Functional parcellation and large-scale reverse inference. Cereb Cortex. 23:739–749.

Chiarello C, Vazquez D, Felton A, Leonard CM. 2013. Structural asymmetry of anterior insula: Behavioral correlates and individual differences. Brain Lang. 126:109–122.

Clark L, Bechara A, Damasio H, Aitken MRF, Sahakian BJ, Robbins TW. 2008. Differential effects of insular and ventromedial prefrontal cortex lesions on risky decision-making. Brain. 131:1311–1322.

Cloutman LL, Binney RJ, Drakesmith M, Parker GJM, Lambon Ralph MA. 2012. The variation of function across the human insula mirrors its patterns of structural connectivity: Evidence from in vivo probabilistic tractography. Neuroimage. 59:3514–3521.

Cohen JD, Mock JR, Nichols T, Zadina J, Corey DM, Lemen L, Bellugi U, Galaburda A, Reiss A, Foundas AL. 2010. Morphometry of human insular cortex and insular volume reduction in Williams syndrome. J Psychiatr Res. 44:81–89.

Collins DL, Holmes CJ, Peters TM, Evans AC. 1995. Automatic 3-D model-based neuroanatomical segmentation. Hum Brain Mapp. 3:190–208.

Côté MA, Girard G, Boré A, Garyfallidis E, Houde JC, Descoteaux M. 2013. Tractometer: Towards validation of tractography pipelines. Med Image Anal. 17:844–857.

Coupe P, Yger P, Prima S, Hellier P, Kervrann C, Barillot C. 2008. An optimized blockwise nonlocal means denoising filter for 3-D magnetic resonance images. IEEE Trans Med Imaging. 27:425–441.

Craig ADB. 2011. Significance of the insula for the evolution of human awareness of feelings from the body. Ann N Y Acad Sci. 1225:72–82.

Crick FC, Koch C. 2005. What is the function of the claustrum? Philos Trans R Soc Lond B Biol Sci. 360:1271–1279.

Dal Monte O, Krueger F, Solomon JM, Schintu S, Knutson KM, Strenziok M, Pardini M, Leopold A, Raymont V, Grafman J. 2013. A voxel-based lesion study on facial emotion recognition after penetrating brain injury. Soc Cogn Affect Neurosci. 8:632–639.

Deen B, Pitskel NB, Pelphrey KA. 2011. Three systems of insular functional connectivity identified with cluster analysis. Cereb Cortex. 21:1498–1506.

Dell'Acqua F, Catani M. 2012. Structural human brain networks: hot topics in diffusion tractography. Curr Opin Neurol. 25:375–383.

Descoteaux M, Deriche R, Knösche TR, Anwander A. 2009. Deterministic and probabilistic tractography based on complex fibre orientation distributions. IEEE Trans Med Imaging. 28:269–286.

Desikan RS, Ségonne F, Fischl B, Quinn BT, Dickerson BC, Blacker D, Buckner RL, Dale AM, Maguire RP, Hyman BT, et al. 2006. An automated labeling system for subdividing the human cerebral cortex on MRI scans into gyral based regions of interest. Neuroimage. 31:968–980.

Dice LR. 1945. Measures of the amount of ecologic association between species. Ecology. 26:297–302.

Dougherty RF, Ben-Shachar M, Bammer R, Brewer AA, Wandell BA. 2005. Functional organization of human occipital-callosal fiber tracts. Proc Natl Acad Sci USA. 102:7350–7355.

Dronkers N. 1996. A new brain region for coordinating speech articulation. Nature. 384:159–161.

Eickhoff SB, Jbabdi S, Caspers S, Laird AR, Fox PT, Zilles K, Behrens TEJ. 2010. Anatomical and functional connectivity of cytoarchitectonic areas within the human parietal operculum. J Neurosci. 30:6409–6421.

Evrard HC, Forro T, Logothetis NK. 2012. Von economo neurons in the anterior insula of the macaque monkey. Neuron. 74:482–489.

Fernández-Miranda JC, Rhoton AL, Kakizawa Y, Choi C, Alvarez-Linera J. 2008. The claustrum and its projection system in the human brain: a microsurgical and tractographic anatomical study. J Neurosurg. 108:764–774.

Flynn FG. 1999. Anatomy of the insula functional and clinical correlates. Aphasiology. 13:55–78.

Frazier JA, Chiu S, Breeze JL, Makris N, Lange N, Kennedy DN, Herbert MR, Bent EK, Koneru VK, Dieterich ME, et al. 2005. Structural brain magnetic resonance imaging of limbic and thalamic volumes in pediatric bipolar disorder. Am J Psychiatry. 162:1256–1265.

Ghaziri J, Tucholka A, Nguyen DK. 2014. The connectivity of the human insular cortex: a review. In: Uddin LQ, editors. Insula: Neuroanatomy, Functions and Clinical Disorders. ed. New York: Nova Scien. p. 31–66.

Girard G, Whittingstall K, Deriche R, Descoteaux M. 2014. Towards quantitative connectivity analysis: Reducing tractography biases. Neuroimage. 98:266–278.

Golay L, Schnider A, Ptak R. 2008. Cortical and subcortical anatomy of chronic spatial neglect following vascular damage. Behav Brain Funct. 4:43.

Goldstein JM, Seidman LJ, Makris N, Ahern T, O'Brien LM, Caviness VS, Kennedy DN, Faraone SV, Tsuang MT. 2007. Hypothalamic abnormalities in schizophrenia: sex effects and genetic vulnerability. Biol Psychiatry. 61:935–945.

Hagmann P, Cammoun L, Gigandet X, Meuli R, Honey CJ, Wedeen VJ, Sporns O. 2008. Mapping the structural core of human cerebral cortex. PLoS Biol. 6:e159.

Hagmann P, Kurant M, Gigandet X, Thiran P, Wedeen VJ, Meuli R, Thiran J-PP. 2007. Mapping human whole-brain structural networks with diffusion MRI. PLoS One. 2:e597.

Ham T, Leff A, de Boissezon X, Joffe A, Sharp DJ. 2013. Cognitive control and the salience network: an investigation of error processing and effective connectivity. J Neurosci. 33:7091–7098.

Heydrich L, Blanke O. 2013. Distinct illusory own-body perceptions caused by damage to posterior insula and extrastriate cortex. Brain. 136:790–803.

Insausti R, Amaral DG, Cowan WM. 1987. The entorhinal cortex of the monkey: II. Cortical afferents. J Comp Neurol. 264:356–395.

Jakab A, Molnár PP, Bogner P, Béres M, Berényi EL. 2012. Connectivity-based parcellation reveals interhemispheric differences in the insula. Brain Topogr. 25:264–271.

Jenkinson M, Beckmann CF, Behrens TEJ, Woolrich MW, Smith SM. 2012. Fsl. Neuroimage. 62:782–790.

Johansen-Berg H, Behrens TEJ. 2006. Just pretty pictures? What diffusion tractography can add in clinical neuroscience. Curr Opin Neurol. 19:379–385.

Jones DK, Knösche TR, Turner R. 2013. White matter integrity, fiber count, and other fallacies: The do's and don'ts of diffusion MRI. Neuroimage. 73:239–254.

Kaas JH. 2013. The evolution of brains from early mammals to humans. Wiley Interdiscip Rev Cogn Sci. 4:33–45.

Karnath HH-O, Baier B. 2010. Right insula for our sense of limb ownership and self-awareness of actions. Brain Struct Funct. 214:411–417.

Karnath H-O, Baier B, Nägele T. 2005. Awareness of the functioning of one's own limbs mediated by the insular cortex? J Neurosci. 25:7134–7138.

Kerr KM, Agster KL, Furtak SC, Burwell RD. 2007. Functional neuroanatomy of the parahippocampal region: the lateral and medial entorhinal areas. Hippocampus. 17:697–708.

Klein A, Andersson J, Ardekani BA, Ashburner J, Avants B, Chiang MC, Christensen GE, Collins DL, Gee J, Hellier P, et al. 2009. Evaluation of 14 nonlinear deformation algorithms applied to human brain MRI registration. Neuroimage. 46:786–802.

Kuhnt D, Bauer MHA, Egger J, Richter M, Kapur T, Sommer J, Merhof D, Nimsky C. 2013. Fiber tractography based on diffusion tensor imaging compared with high-angular-resolution diffusion imaging with compressed sensing: Initial experience. Neurosurgery. 72:165–175.

Kurth F, Zilles K, Fox PT, Laird AR, Eickhoff SB. 2010. A link between the systems: functional differentiation and integration within the human insula revealed by meta-analysis. Brain Struct Funct. 214:519–534.

Makris N, Goldstein JM, Kennedy D, Hodge SM, Caviness VS, Faraone SV, Tsuang MT, Seidman LJ. 2006. Decreased volume of left and total anterior insular lobule in schizophrenia. Schizophr Res. 83:155–171.

Manes F, Paradiso S, Robinson R. 1999. Neuropsychiatric effects of insular stroke. J Nerv. 187:1–11.

Martino J, Brogna C, Robles SG, Vergani F, Duffau H. 2010. Anatomic dissection of the inferior fronto-occipital fasciculus revisited in the lights of brain stimulation data. Cortex. 46:691–699.

Mathur BN. 2014. The claustrum in review. Front Syst Neurosci. 8:48.

Mazziotta J, Toga A, Evans A, Fox P, Lancaster J, Zilles K, Woods R, Paus T, Simpson G, Pike B, et al. 2001. A probabilistic atlas and reference system for the human brain: International Consortium for Brain Mapping (ICBM). Philos Trans R Soc Lond B Biol Sci. 356:1293–1322.

Menon V, Uddin LQ. 2010. Saliency, switching, attention and control: a network model of insula function. Brain Struct Funct. 214:655–667.

Mesulam MM, Mufson EJ. 1982a. Insula of the old world monkey. I. Architectonics in the insulo-orbito-temporal component of the paralimbic brain. J Comp Neurol. 212:1–22.

Mesulam MM, Mufson EJ. 1982b. Insula of the old world monkey. III: Efferent cortical output and comments on function. J Comp Neurol. 212:38–52.

Mesulam MM, Mufson EJ. 1985. The insula of Reil in man and monkey. In: Peters A, Jones EG, editors. Association and Auditory Cortices. Cerebral Cortex. Boston (MA): Springer US. p. 179–226.

Morris DM, Embleton KV, Parker GJM. 2008. Probabilistic fibre tracking: Differentiation of connections from chance events. Neuroimage. 42:1329–1339.

Mufson EJ, Mesulam MM. 1982. Insula of the old world monkey. II: Afferent cortical input and comments on the claustrum. J Comp Neurol. 212:23–37.

Mutschler I, Wieckhorst B, Kowalevski S, Derix J, Wentlandt J, Schulze-Bonhage A, Ball T. 2009. Functional organization of the human anterior insular cortex. Neurosci Lett. 457:66–70.

Naidich TP, Kang E, Fatterpekar GM, Delman BN, Gultekin SH, Wolfe D, Ortiz O, Yousry I, Weismann M, Yousry TA. 2004. The Insula: Anatomic Study and MR Imaging Display at 1.5 T. Am J Neuroradiol. 25:222–232.

Nieuwenhuys R. 2012. The insular cortex. A review. 1st ed. Progress in Brain Research. Elsevier B.V.

Nieuwenhuys R, Voogd F, Van Hujzen C. 1988. The human central nervous system. ed. Berlin: Springer.

Nimchinsky EA, Vogt BA, Morrison JH, Hof PR. 1995. Spindle neurons of the human anterior cingulate cortex. J Comp Neurol. 355:27–37.

Pandya DN, Van Hoesen GW, Mesulam MM. 1981. Efferent connections of the cingulate gyrus in the rhesus monkey. Exp Brain Res. 42:319–330.

Raffelt D, Tournier JD, Rose S, Ridgway GR, Henderson R, Crozier S, Salvado O, Connelly A. 2012. Apparent Fibre Density: A novel measure for the analysis of diffusion-weighted magnetic resonance images. Neuroimage. 59:3976–3994.

Room P, Groenewegen HJ. 1986. Connections of the parahippocampal cortex. I. Cortical Afferents. J Comp Neurol. 251:415–450.

Schmahmann JD, Pandya DN. n.d.. The complex history of the fronto-occipital fasciculus. J Hist Neurosci. 16:362–377.

Schmahmann JD, Pandya DN, Wang R, Dai G, D'Arceuil HE, De Crespigny AJ, Wedeen VJ. 2007. Association fibre pathways of the brain: Parallel observations from diffusion spectrum imaging and autoradiography. Brain. 130:630–653.

Seeley WW, Menon V, Schatzberg AF, Keller J, Glover GH, Kenna H, Reiss AL, Greicius MD. 2007. Dissociable intrinsic connectivity networks for salience processing and executive control. J Neurosci. 27:2349–2356.

Semendeferi K, Damasio H. 2000. The brain and its main anatomical subdivisions in living hominoids using magnetic resonance imaging. J Hum Evol. 38:317–332.

Shelley BP, Trimble MR. 2004. The insular lobe of Reil–its anatamico-functional, behavioural and neuropsychiatric attributes in humans–a review. World J Biol Psychiatry. 5:176–200.

Shipp S, Blanton M, Zeki S. 1998. A visuo-somatomotor pathway through superior parietal cortex in the macaque monkey: Cortical connections of areas V6 and V6A. Eur J Neurosci. 10:3171–3193.

Smith RE, Tournier JD, Calamante F, Connelly A. 2012. Anatomically-constrained tractography: Improved diffusion MRI streamlines tractography through effective use of anatomical information. Neuroimage. 62:1924–1938.

Smith SM. 2002. Fast robust automated brain extraction. Hum Brain Mapp. 17:143–155.

Smith SM, Jenkinson M, Woolrich MW, Beckmann CF, Behrens TEJ, Johansen-Berg H, Bannister PR, De Luca M, Drobnjak I, Flitney DE, et al. 2004. Advances in functional and structural MR image analysis and implementation as FSL. Neuroimage. 23:208–219.

Stephani C, Fernandez-Baca Vaca G, MacIunas R, Koubeissi M, Lüders HO. 2011. Functional neuroanatomy of the insular lobe. Brain Struct Funct. 216:137–149.

Tamraz JC, Comair YG, Edition S. 2004. Atlas of Regional Anatomy of the Brain using MRI. Berlin: Springer.

Tanné-Gariépy J, Rouiller EM, Boussaoud D. 2002. Parietal inputs to dorsal versus ventral premotor areas in the macaque monkey: Evidence for largely segregated visuomotor pathways. Exp Brain Res. 145:91–103.

Tanriover N, Rhoton AL, Kawashima M, Ulm AJ, Yasuda A. 2004. Microsurgical anatomy of the insula and the sylvian fissure. J Neurosurg. 100:891–922.

Taylor KS, Seminowicz DA, Davis KD. 2009. Two systems of resting state connectivity between the insula and cingulate cortex. Hum Brain Mapp. 30:2731–2745.

Torta DM, Cauda F. 2011. Different functions in the cingulate cortex, a meta-analytic connectivity modeling study. Neuroimage. 56:2157–2172.

Tournier JD, Calamante F, Connelly A. 2007. Robust determination of the fibre orientation distribution in diffusion MRI: Non-negativity constrained super-resolved spherical deconvolution. Neuroimage. 35:1459–1472.

Tournier JD, Calamante F, Connelly A. 2012. MRtrix: Diffusion tractography in crossing fiber regions. Int J Imaging Syst Technol. 22:53–66.

Tournier J-D, Yeh C-H, Calamante F, Cho K-H, Connelly A, Lin C-P. 2008. Resolving crossing fibres using constrained spherical deconvolution: validation using diffusion-weighted imaging phantom data. Neuroimage. 42:617–625.

Türe U, Yaşargil DC, Al-Mefty O, Yaşargil MG. 1999. Topographic anatomy of the insular region. J Neurosurg. 90:720–733.

Tzourio-Mazoyer N, Landeau B, Papathanassiou D, Crivello F, Etard O, Delcroix N, Mazoyer B, Joliot M. 2002. Automated anatomical labeling of activations in SPM using a macroscopic anatomical parcellation of the MNI MRI single-subject brain. Neuroimage. 15:273–289.

Uddin LQ, Supekar K, Amin H, Rykhlevskaia E, Nguyen DA, Greicius MD, Menon V. 2010. Dissociable connectivity within human angular gyrus and intraparietal sulcus: evidence from functional and structural connectivity. Cereb Cortex. 20:2636–2646.

Van Den Heuvel MP, Mandl RCW, Kahn RS, Hulshoff Pol HE. 2009. Functionally linked resting-state networks reflect the

underlying structural connectivity architecture of the human brain. Hum Brain Mapp. 30:3127–3141.

Vincent JL, Kahn I, Snyder AZ, Raichle ME, Buckner RL. 2008. Evidence for a frontoparietal control system revealed by intrinsic functional connectivity. J Neurophysiol. 100: 3328–3342.

Vogt BA, Nimchinsky EA, Vogt LJ, Hof PR. 1995. Human cingulate cortex: Surface features, flat maps, and cytoarchitecture. J Comp Neurol. 359:490–506.

Vogt BA, Pandya DN. 1987. Cingulate cortex of the rhesus monkey: II. Cortical afferents. J Comp Neurol. 262:271–289.

Vogt BA, Pandya DN, Rosene DL. 1987. Cingulate cortex of the rhesus monkey: I. Cytoarchitecture and thalamic afferents. J Comp Neurol. 262:256–270.

von Economo C. 1926. Eine neue art spezialzellen des lobus cinguli und lobus insulae. Zeitschrift für die Gesamte Neurol und Psychiatr. 100:706–712.

von Economo CF, Koskinas G. 1925. Die cytoarchitektonik der hirnrinde des erwachsenen menschen. Berlin: J. Springer.

Weller JA, Levin IP, Shiv B, Bechara A. 2009. The effects of insula damage on decision-making for risky gains and losses. Soc Neurosci. 4:347–358.

Woolrich MW, Jbabdi S, Patenaude B, Chappell M, Makni S, Behrens T, Beckmann C, Jenkinson M, Smith SM. 2009. Bayesian analysis of neuroimaging data in FSL. Neuroimage. 45:S173–S186.

Yo T-S, Anwander A, Descoteaux M, Fillard P, Poupon C, Knösche TR. 2009. Quantifying brain connectivity: a comparative tractography study. Med Image Comput Comput Assist Interv. 12:886–893.

Yushkevich PA, Piven J, Hazlett HC, Smith RG, Ho S, Gee JC, Gerig G. 2006. User-guided 3D active contour segmentation of anatomical structures: Significantly improved efficiency and reliability. Neuroimage. 31:1116–1128.

Zalesky A, Fornito A, Harding IH, Cocchi L, Yücel M, Pantelis C, Bullmore ET. 2010. Whole-brain anatomical networks: Does the choice of nodes matter? Neuroimage. 50:970–983.

Zhang Y, Brady M, Smith S. 2001. Segmentation of brain MR images through a hidden Markov random field model and the expectation-maximization algorithm. IEEE Trans Med Imaging. 20:45–57.